The use of microbial and chemical analyses to characterize the variations in fouling profile of seawater reverse osmosis (SWRO) membrane

Carmem-Lara de O. Manes[a,1], Muhammad Tariq Khan[a,1], Veronica Garcia Molina[b], Jean-Philippe Croue[a,*]

[a]*Water Desalination and Reuse Center, King Abdullah University of Science and Technology (KAUST), Thuwal 23955-6900, Kingdom of Saudi Arabia*
[b]*Dow Water and Process Solutions, Autovía Tarragona-Salou s/n, Tarragona 43006, Spain*

ABSTRACT

Biofouling of reverse osmosis (RO) membranes is one of the most common problems in desalinations plants reducing the efficiency of the water production process. The characterization of bacterial community composition from fouling layers as well as detailed analysis of surrounding chemical environment might reveal process specific bacterial groups/species that are involved in RO biofouling. In this study, advanced organics analytic methods (elemental analysis, FTIR, and ICP-OES) were combined with high-throughput 16S rRNA (pyro) sequencing to assess in parallel, the chemical properties and the active microbial community composition of SWRO membranes from a pilot desalination plant (MFT, Tarragona) in February 2011 and July 2011. Prefiltered ultrafiltration. waters fed SWRO membranes during third and fifth month of operation, respectively. SWRO samples were taken from three modules at different positions (first, fourth, and sixth) in order to investigate the spatial changes in fouling layers' chemical and microbiological composition. The overall assessment of chemical parameters revealed that fouling layers were mainly composed by bio and organic material (proteins and lipids). Ca and Fe were found to be the most abundant elements having an increasing concentration gradient according to the module position. Bacterial community composition of SWRO membranes is mostly represented by the Gammaproteobacteria class with interesting differences in genera/species spatial and temporal distribution. This preliminary result suggests that pretreatments and/or operational conditions might have selected different bacterial groups more adapted to colonize SWRO membranes.

Keywords: Water pretreatment; Reverse osmosis membrane; Fouling; Biopolymers; Microbial community

1. Introduction

Seawater reverse osmosis (SWRO) fouling phenomenon is complex and multifactorial. Apart from inorganic and scaling problems it is known that biofouling is the most common and detrimental kind of fouling within the desalination process as it cannot be avoided by conventional pretreatment procedures [1]. Biofouling includes organic matter deposition and microbial growth on the SWRO surface. Today some

*Corresponding author.
[1]These authors contributed equally to this work.

scientists are trying to tackle the SWRO biofouling phenomenon by investigating its origin and development. However, none have yet applied combined advanced methods to better understand the interactions between the composition of fouling layers and the diversity and dynamics of living microbial community within it. It is likely that the accumulation of certain organic compounds would select certain microbes that would participate in the fouling layer development more actively than others and this hypothesis is investigated in this paper. To better understand the biofouling process it is important to compare at different time points the microbial communities on the SWRO membranes and also the eventual effect that module position might exert over membrane bacterial community. We have applied advanced analytical tools comprising elemental analysis, FTIR, and ICP-OES combined to next generation sequencing of 16S rRNA to assess in parallel, the chemical properties and the microbial diversity of SWRO membranes from a pilot desalination plant at DOW facilities (MFT, Tarragona, Spain) in February 2011 and August 2011.

2. Methods

2.1. Samples and Site Description

The SWRO pilot unit, located in Tarragona- Spain, has 6 inch RO (FILMTEC™ SW30XLE-4040) modules with pretreatment setup comprising of Amiad filter 50 micron and ultrafiltration (DOW UF™ SFP-2660). Each reverse osmosis (RO) line consists of pressure vessels with six elements in series. The seawater intake is from the harbor of the city (Mediterranean Sea). A 10 km long pipe connects the intake with the desalination facility and it is provided with an Arkal ring filter (250 micron). Average quality of the seawater entering the unit was below 3 NTU of turbidity and below 10 mg/L of TSS although peaks up to 15 NTU and 50 mg/L have been punctually monitored. Feedwater temperature ranged from 13 to 30 °C between the sampling periods.

A total of six SWRO membranes were taken from three modules at different positions (first, fourth, and sixth) within the process line at two sampling periods T1 (February 2011) and T2 (August 2011). FILMTEC™ SWRO membranes were fed by prefiltered UF (0.03 micron) water. The membranes were in use for three (T1) and five (T2) months.

2.2. Fouling load and chemical analysis

Foulant material was collected from the fouled membrane sheets by physical scrapping. Dried foulant material was obtained through lyophilization process.

Recovered foulant mass was weighed and mass per area of the fouled membrane (fouling load) was calculated.

2.2.1. Loss on ignition (LOI) test

Lyophilized foulant material samples were dehydrated overnight at 105 °C and then accurately weighed quantities (10–30 mg), taken in fused quartz crucibles, were subjected to ignition at 550 °C in muffle furnace for four hours. Percentage loss on ignition was calculated in the following way [2].

$$\% \, LOI = Weight(Dry) - Weight(@ \, 550 \, °C)/Weight(Dry)$$

2.2.2. Elemental analysis

Accurately weighed amount of samples (15–20 mg) was digested with 1 ml of trace metal analysis grade HNO_3, diluted to 20 ml with ultrapure water. Clear solution obtained after digestion and dilution was analyzed with ICP-OES for concentration of inorganic elements.

Flash 2000—Thermo Scientific CHNS/O Analyzer was used for CHNS of predried and well powdered foulant material following the US-EPA 440.0 analytical method [3].

2.2.3. Fourier transform infra-red (FT-IR) spectroscopy

The IR spectrometer "Spectrum 100 FTIR" by PerkinElmer was used for analysis. Potassium bromide (KBr) pellet method was used which involved the mixing and grinding of approximately 200–300 μg of dried sample with 100 mg of KBr salt. Considerably transparent and thin (about 0.5 mm in thickness) pellets were formed after submitting the mixture to the press of 10 tons/in². Each of the obtained spectra was average of 20 scans at resolution of 1 cm⁻¹ with scanning range from 4,000–400 cm⁻¹.

2.3. Microbial analysis

2.3.1. Nucleic acids extraction and next generation sequencing and taxonomic classification analysis

DNA extraction, next generation sequencing, and taxonomic classification analysis were performed by the method and technique stated by Manes et al. [4].

Pyrosequencing of the total genomic DNA extracted from water and membrane samples of this study was obtained from the Research and Testing Laboratory facility (TX, USA) as published by Dowd

et al. (2008) [5] in a Roche 454 FLX Genome Sequencer. Bacterial 16S rDNA was sequenced using primer 27F (5′-AGAGTTTGATCMTGGCTCAG-3′) and reverse primer 519R 5′ GTNTTACNGCGGCKGCTG targeting the V2-V3 variable regions. Sequence data-set was preprocessed in RTL facilities in order to reduce the noise and sequencing artifacts including searching for chimeras and clustering according to Dowd et al. (2008) [6].

Bacterial diversity of the remaining sequence data-set (average >3,000 sequences per sample) was queried against a database of high-quality 16S sequences derived from NCBI (current version) and analyzed statistically with the PAST software [7]. The beta diversity of the sequence data-set was analyzed using Bray Curtis algorithm taking into account operational taxonomic unit abundances and distribution.

3. Results and discussion

3.1. Characterization of the fouling layer composition

3.1.1. Nature of the foulant material and elemental analysis

T1 modules (operated for three months) presented a lower fouling load; 0.01–0.38 g/m^2 than the T2 modules (operated for five months); 0.01–0.77 g/m^2. Chemical analysis results showed similarity in the

fouling trend among the two sets of modules i.e. fouling load was gradually decreased from the first module to the sixth module position in both sets (Table 1). For all samples, the foulant material was mainly composed of organic matter and the proportion of organics in T1 and T2 modules also gradually decreased from the first (92 and 89.17%, respectively) to sixth module position (81.3 and 75%, respectively). The elevated organic contents of all foulant samples indicated that the pilot was subjected to organic fouling and/or biofouling (Table 1). Furthermore, the nature of the organic foulant material could be inferred by the C/N and H/C ratio values. A relatively low C/N ratio (6.5–7.9) was observed for all the studied samples and this value was found to increase from the first to last position module at both time points, T1 and T2 (Table 1). This result suggests that the foulant material of the first module was richer in proteinaceous substances according to Meyers [8,9] which might be originated from the microbial activity. The H/C atomic ratio ranging from 1.52 to 1.77 for all samples suggests a predominance of aromatic organic matter, such as humic substances, in their foulant material [10]. Hedges and collaborators have reported the C/H ratios ranging from 1.21 to 1.57 in the marine dissolved humic substances [11]. Particularly, the presence of aromatic substances is more pronounced in the foulant material of modules which is supposed to

Table 1
Comparative analysis of fouling profile of the two set of autopsies

Analysis	Element	Unit	T1			T2		
			M1	M4	M6	M1	M4	M6
Fouling Load		g/m^2	0.38	0.043	0.013	0.774	0.052	0.014
Loss on Ignition	LOI	%	92.38	87.1	81.3	89.17	87.25	75.00
	Residue		7.62	12.9	18.7	10.83	12.75	25.00
CHNS	C	Weight %	45.43	43.44	40.11	41.29	42.77	46.81
	H		6.63	6.25	5.09	6.07	6.18	6.04
	N		7.76	6.41	6.02	7.39	7.39	6.9
	S		0.98	1.03	1.01	2.00	1.95	2.06
	C/N	Atomic ratio	6.85	7.90	7.77	6.51	6.75	7.91
	H/C		1.73	1.72	1.52	1.77	1.73	1.56
ICP-OES	Al	mg/g	0.11	0.50	1.13	0.12	0.39	1.44
	Ca		5.85	8.53	19.38	6.02	9.14	51.10
	Fe		1.56	8.30	9.38	2.67	3.52	7.96
	Mg		1.89	1.20	3.38	2.40	2.47	1.86
	P		0.04	0.20	0.13	8.40	6.33	5.76
	S		7.11	6.18	2.63	20.58	14.17	12.54
	Si		5.52	4.33	2.88	0.12	0.65	1.69

be in the initial phase of the fouling layer formation as T1M6 and T2M6 (H/C = 1.52 and 1.56, respectively). This is an indication of role of these aromatic substances, e.g. humic substances, in the membrane surface conditioning which is an initial step in the biofouling phenomenon.

ICP-OES elemental analysis on the foulant material of all samples revealed significant presence of multivalent cations i.e. Ca and Fe (Table 1), which are known for their probable role in stabilizing the organic substances through the mitigation of the electrostatic repulsion among the negatively charged moieties of these organics. The dominance of sulfur especially in T2 samples might be attributed to sulfite dosing employed at the pilot plant as a pretreatment for dechlorination of water before RO inlet.

3.1.2. Organic matter characterization of foulant materials

Equal amount of samples was subjected to IR analysis and the intensities of the signals for organic matter of the foulant material of T1 membranes were lower as compared to that of T2 membranes demonstrating that more organic matter was accumulated on T2 membranes (Fig. 1). Moreover, the intensities of these signals within both sets of membranes were observed to decrease from M1 to M6 foulant material, which revealed that the fouling layer was compara-

tively less developed on the modules located after the lead position, i.e. M4 and M6.

In the IR spectra, proteins were indicated by amide A (N–H, $3,300 \, cm^{-1}$), amide I $1,652 \, cm^{-1}$ (N–C=O, 1,652), and amide II (N=C–O, $1,548 \, cm^{-1}$) signals. A major band located near $1,050 \, cm^{-1}$ (C–O and C–O–C) pointed the presence of sugars and a peak at $1,380 \, cm^{-1}$ revealed the amino sugars (CH_3 of N-acetyl group). The presence of lipids was suggested by bands at $2,960 \, cm^{-1}$, $2,925 \, cm^{-1}$, and $2,850 \, cm^{-1}$ [12]. Additionally, a COOR band at $1,735 \, cm^{-1}$ and CH_2 band at $1,415 \, cm^{-1}$ also indicated the presence of lipids [13]. The signal at $1,380 \, cm^{-1}$ is attributed to amino sugars, the degradation product of bacterial cell wall peptidoglycans. A sharp peak close to $1,380 \, cm^{-1}$ could be attributed to inorganic nitrates and/or aliphatic nitro compounds [12,14]. This peak was only observed in the IR spectra of foulant material of T2 membranes. The band at $1,240 \, cm^{-1}$ is attributable to the stretching vibration of phosphodiester backbone of the nucleic acid indicating the presence of DNA/RNA molecules [15].

3.2. Microbial diversity and dynamics

3.2.1. Temporal changes in SWRO membrane bacterial community structure

To determine the bacterial diversity on the membrane samples, high-throughput 16S rRNA gene sequencing was performed. This analysis not only allowed an evaluation of the identity of bacterial groups present on the membranes at two time points with a year on site but also could give clues as to the differences in their spatial distribution within module positions.

At T1, the most abundant affiliated phylotypes belonged to the *Proteobacteria* followed by *Bacteroidetes* phyla. Members of *Alphaproteobacteria* and *Gammaproteobacteria* classes almost exclusively represented the *Proteobacteria* phylum. Moreover, the different phyla were fairly evenly distributed among the samples from modules one, four, and six (Fig. 2) and diversity index was relatively low: Shannon-H = 2,196 (M1), 2,126 (M4), and 1,874 (M6), respectively. A clear community distribution shift could be seen at T2. Although *Proteobacteria* phylum was the most represented phylum from the three membranes, *Bacteroidetes*, *Firmicutes* and *Planctomycetes* phyla were also represented and particularly for M1 at relatively high abundances. Within, *Proteobacteria*, *Alphaproteobacteria* and *Betaproteobacteria* were shown to be the most commonly represented in M4 and M6 samples, however, *Gammaproteobacteria* was the most abundant
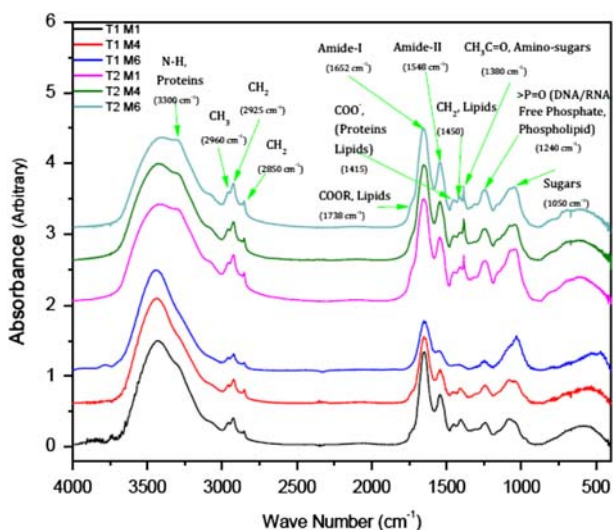
Fig. 1. IR spectra of foulant materials from SWRO membranes (M) located at different module positions in a pilot desalination plant. T1, first autopsy time point during February 2011; T2, second autopsy time point during August 2011; 1–6 module positions within the pilot process line.
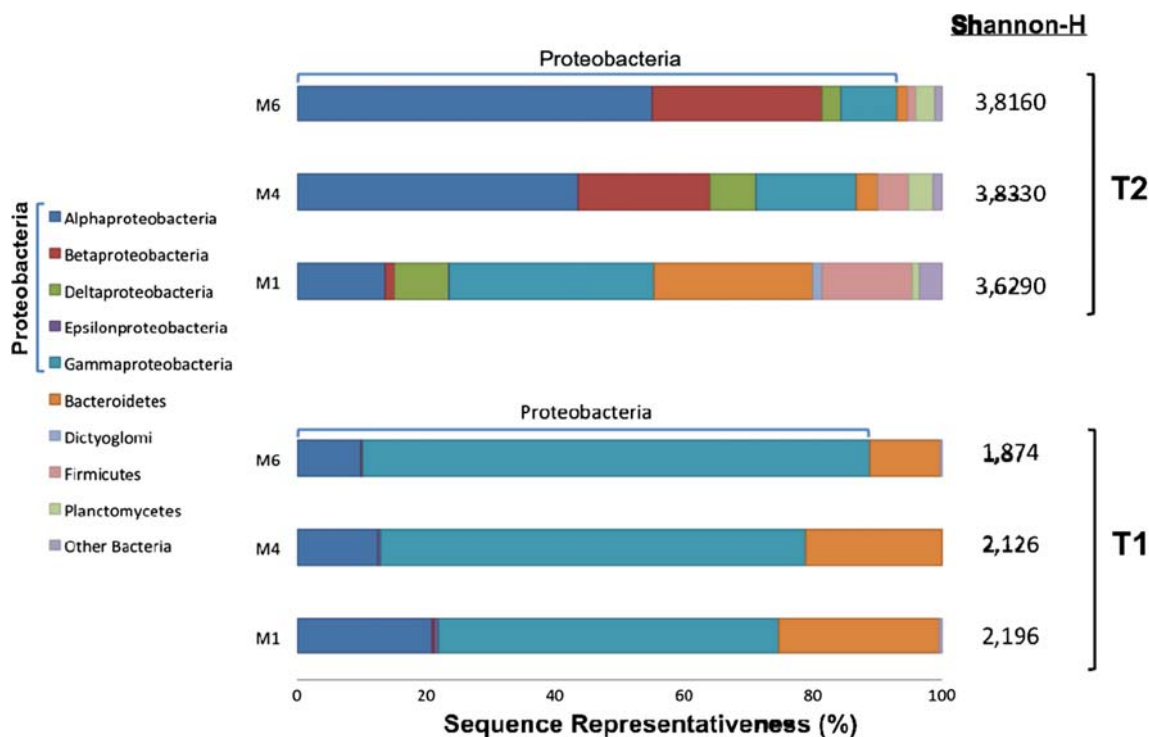
Fig. 2. Schematic representation of the hierarchical classification and distribution of the 16S ribosomal RNA gene sequence data-sets into major bacterial Phyla and *Proteobacteria* classes. Shannon-H diversity index is depicted at the right hand column for each sample.

in M1. The highest diversity of phylotypes encountered on T2 samples is corroborated by an elevated diversity index >3.6 (Shannon-H) measured for the three of them (Fig. 2). It is likely that diversity increases with SWRO membrane usage time and this is consistent to a previously described bacterial diversity analysis of SWRO membranes from a full-scale desalination plant, where the membrane in use for longer periods were more diverse than the ones used for few weeks (Shannon-H = 3.7 against 2.2, respectively) [4].

Regarding the spatial distribution of phylotypes among the modules at T1 and T2, it was observed that the bacterial community structure of T1 membranes was very alike whereas clear differences from M1 to M4 and M6 were observed for T2 membranes. This is an interesting observation, and to our knowledge, not yet described. It might be possible that SWRO membrane bacterial community structure at the first position is the one that would change more often than other ones due to water quality changing parameters. This would work as a prefilter selecting some bacterial groups for the other modules in the process line. The direct link between the organic matter composition and bacterial community composition remains to be unraveled.

References

[1] C.-L. de O. Manes, C. Barbe, N. West, S. Rapenne, P. Lebaron, Impact of seawater-quality and water treatment procedures on the active bacterial assemblages at two desalination sites, Environ. Sci. Technol. 45(14) (2011) 5943–5951.

[2] O. Heiri, André F. Lotter, G. Lemcke, Loss on ignition as a method for estimating organic and carbonate content in sediments: Reproducibility and comparability of results, J. Paleolimnol. 25 (2001) 101–110.

[3] US-EPA Method 440.0, Determination of Carbon and Nitrogen in sediments and particulates of estuarine/coastal waters using elemental analysis, 1997.

[4] C.-L. de O. Manes, N. West, S. Rapenne, P. Lebaron, Dynamic bacterial communities on reverse-osmosis membranes in a full-scale desalination plant. GBIF 27 (2011) 47–58.

[5] S.E. Dowd, T.R. Callaway, R.D. Wolcott, Y. Sun, T. McKeehan, R.G. Hagevoort, T.S. Edrington, Evaluation of the bacterial diversity in the feces of cattle using 16S rDNA bacterial tag-encoded FLX amplicon pyrosequencing (bTEFAP), BMC Microbiol. 8 (2008) 125.

[6] S.E. Dowd, Y. Sun, P.R. Secor, D.D. Rhoads, B.M. Wolcott, G. A. James, R.D. Wolcott, Survey of bacterial diversity in chronic wounds using Pyrosequencing, DGGE, and full ribosome shotgun sequencing, BMC Microbiol. 8 (2008) 43.

[7] Ø. Hammer, D.A.T. Harper, D.R. Paul, Past: paleontological statistics software package for education and data analysis. Palaeontol. Electronica 4 (2001) 9. Available from: http://folk.uio.no/ohammer/past/.

[8] P.A. Meyers, Preservation of elemental and isotopic source identification of sedimentary organic matter, Chem. Geol. 114 (3–4) (1994) 289–302.

[9] P.A. Meyers, Organic geochemical proxies of paleoceanographic, paleolimnologic, and paleoclimatic processes, Org. Geochem. 27(5–6) (1997) 213–250.

[10] J.J. Alberts, M. Takács, Characterization of natural organic matter from eight Norwegian surface waters: The effect of ash on molecular size distributions and CHN content, Environ. Int. 25(2–3) (1999) 237–244.

[11] J.I. Hedges, P.G. Hatcher, J.R. Ertel, K.J. Meyers-Schulte, A comparison of dissolved humic substances from seawater with amazon river counterparts by 13c-nmr spectrometry, Geochim. Cosmochim. Acta 56(4) (1992) 1753–1757.

[12] M. Igisu, Y. Ueno, M. Shimojima, S. Nakashima, S.M. Awramik, H. Ohta, S. Maruyama, Micro-FTIR spectroscopic signatures of bacterial lipids in proterozoic microfossils, Precambrian Res. 173(1–4) (2009) 19–26.

[13] J.A. Leenheer, Systematic approaches to comprehensive analyses of natural organic matter, Ann. Environ. Sci. 3 (2009) 1–130.

[14] J. Coates, Interpretation of infrared spectra, a practical approach, in: R.A. Meyers (Ed.), Encyclopedia of Analytical Chemistry, John Wiley & Sons, Chichester, 2000, pp. 10815–10837.

[15] D. Naumann, C. Schultz, D. Helm, What can infrared spectroscopy tell us about the structure and composition of intact bacterial cells? in: H.H. Mantsch, D. Chapman (Eds), Infrared Spectroscopy of Biomolecules, John Wiley & Sons, New York, NY, 1996, pp. 279–310.